

ASPHALT PAVEMENTS



DEVENDRA DAMALE

Asphalt Pavements

Editor

Devendra Damale


scitus
academics

Asphalt Pavements

Edited by **Devendra Damale**

ISBN: 978-1-68117-013-8

Library of Congress Control Number: 2015931397

© 2016 by

SCITUS Academics LLC,

www.scitusacademics.com

Box No. 4766, 616 Corporate Way,

Suite 2, Valley Cottage,

NY 10989

This book contains information obtained from highly regarded resources. Copyright for individual articles remains with the authors as indicated. All chapters are distributed under the terms of the Creative Commons Attribution License, which permits unrestricted use, distribution, and reproduction in any medium, provided the original author and source are credited.

Notice

Reasonable efforts have been made to publish reliable data and views articulated in the chapters are those of the individual contributors, and not necessarily those of the editors or publishers. Editors or publishers are not responsible for the accuracy of the information in the published chapters or consequences of their use. The publisher believes no responsibility for any damage or grievance to the persons or property arising out of the use of any materials, instructions, methods or thoughts in the book. The editors and the publisher have attempted to trace the copyright holders of all material reproduced in this publication and apologize to copyright holders if permission has not been obtained. If any copyright holder has not been acknowledged, please write to us so we may rectify.

Printed in United States of America on Acid Free Paper ∞

Preface

Asphalt pavements are easy to maintain, quick to construct, and provide a safe, smooth, quiet ride. Simply put, asphalt pavements provide the greatest level of drivability at the most economical price. Asphalt pavement refers to any paved road surfaced with asphalt. Hot Mix Asphalt (HMA) is a combination of approximately 95% stone, sand, or gravel bound together by asphalt cement, a product of crude oil. Asphalt cement is heated aggregate, combined, and mixed with the aggregate at an HMA facility. Asphalt is America's most recycled material. Reclaimed asphalt is not just reusable as a "black rock" – the asphalt cement in the reclaimed pavement is reactivated to become an integral part of the new pavement. The recycled asphalt cement replaces part of the new asphalt cement required for the pavement, reducing costs for road agencies. Recycling is just one reason that asphalt is the most sustainable pavement. Asphalt pavements that are designed and constructed as Perpetual Pavements never need to be removed and replaced. They are permanent structures. The only maintenance needed is infrequent replacement of the surface – and the material that is removed is recycled. This book focuses on asphalt pavement management, processes, operations, methods and techniques. Asphalt recycling also has been pointed out.

Editor

Contents

	Preface.....vii
Chapter 1	Road Asphalt Pavements Analyzed by Airborne Thermal Remote Sensing: Preliminary Results of the Venice Highway 1
	Simone Pascucci, Cristiana Bassani, Angelo Palombo, Maurizio Poscolieri and Rosa Cavalli
Chapter 2	Performance of Recycled Asphalt Pavement as Coarse Aggregate in Concrete.....29
	Fidelis O. OKAFOR
Chapter 3	Effects of Diurnal Temperature Dynamics on Curing of Cold-Emulsion Reclaimed Asphalt Pavements45
	Kiplagat Chelelgo
Chapter 4	Comparative Structural Analysis of Flexible Pavements Using Finite Element Method..... 63
	Ankit Gupta, Abhinav Kumar
Chapter 5	Evaluation of Hot Mix Asphalt Mixtures With Replacement of Aggregates by Reclaimed Asphalt Pavement (RAP) Material79
	O. Reyes-Ortiz, E. Berardinelli, A.E. Alvarez, J.S. Carvajal-Muñoz and L.G. Fuentes
Chapter 6	Performance Characteristics of Fiber Modified Asphalt Concrete Mixes.97
	Manoj Shukla/Dr. Devesh Tiwari/K. Sitaramanjaneyulu
Chapter 7	Experimental Analysis of Waterproofing Polymeric Pavements for Concrete Bridge Decks..... 115
	Marco Pasetto/Giovanni Giacomello

Chapter 8	Thermal Stability Analysis under Embankment with Asphalt Pavement and Cement Pavement in Permafrost Regions ..	139
	Zhang Junwei, Li Jinping, and Quan Xiaojuan	
Chapter 9	Effects of Crumb Rubber Size and Concentration on Performance of Porous Asphalt Mixtures.....	171
	Altan Cetin	
Chapter 10	Landscape Engineering, Protecting Soil, and Runoff Storm Water	197
	Mehmet Cetin	
Chapter 11	Method of Quantification of Hydrated Lime in Asphalt Mixtures.....	233
	V. Mouilleta, D. Séjournéa, V. Delmottea, H.-J. Ritterb, and D. Lesueur	
Chapter 12	Recycled Tyre Rubber Modified Bitumens for Road Asphalt Mixtures: A Literature Review	255
	Davide Lo Presti*	
	Citations.....	313
	Index.....	317

Road Asphalt Pavements Analyzed by Airborne Thermal Remote Sensing: Preliminary Results of the Venice Highway

Simone Pascucci^{1,*}, Cristiana Bassani², Angelo Palombo¹, Maurizio Poscolieri³ and Rosa Cavalli²

¹National Research Council, Institute of Methodologies for Environmental Analysis, C.da S. Loja -Zona Industriale, Tito Scalo (PZ), 85050, Italy

²National Research Council, Institute of Atmospheric Pollution, Via Fosso del Cavaliere, 100, Roma, 00133, Italy

³National Research Council, IDAC, Via Fosso del Cavaliere, 100, Roma, 00133, Italy

ABSTRACT

This paper describes a fast procedure for evaluating asphalt pavement surface defects using airborne emissivity data. To develop this procedure, we used airborne multispectral emissivity data covering an urban test area close to Venice (Italy). For this study, we first identify and select the roads' asphalt pavements on Multispectral Infrared Visible Imaging Spectrometer (MIVIS) imagery using a segmentation procedure. Next, since in asphalt pavements the surface defects are strictly related to the decrease of oily components that cause an increase of the abundance of surfacing limestone, the diagnostic absorption emissivity peak at $11.2\mu\text{m}$ of the limestone was used for retrieving from MIVIS emissivity data the areas exhibiting defects on asphalt pavements surface. The results showed that MIVIS emissivity allows establishing a threshold that points out those asphalt road sites on which a check for a maintenance intervention is required. Therefore, this technique can supply local government authorities an efficient, rapid and repeatable road mapping procedure providing the location of the asphalt pavements to be checked.

INTRODUCTION

According to the European Asphalt Pavement Association (EAPA; <http://www.eapa.org/>), asphalt pavement is commonly referred to as a mixture of bitumen and mineral matter [12,48] that for Italy asphalts is mainly composed of silicates and limestone [2]. The primary surface defects that occur on the asphalt pavement mixture are raveling, flushing and polishing [67]. Raveling is defined as "the progressive loss of pavement material from the asphalt surface caused by (a) stripping of the bituminous film from the aggregate, (b) asphalt hardening due to aging, (c) poor compaction especially or insufficient asphalt content". Flushing is the "excess asphalt on the surface caused by a poor initial asphalt mix design". Polishing is defined as "a smooth oily surface caused by traffic wearing off sharp edges of aggregates" [67].

The management and maintenance of transportation infrastructures are based on detailed and accurate information about the road network. The pavement type and road surface conditions are the most common variables required to provide detailed road mapping. This data is critical

to the management decision process that involves billions of euros of assets, and maintenance budgets of millions of euros each year. Moreover, street maintenance work looks still today like something hurriedly thrown and only based on the roadman job. Often the maintenance is carried out when the pavement is approaching its collapse point and with renewal interventions linked to the worker experience [57].

Remote sensing can solve the road condition mapping by applying relatively cheap methods to evaluate the surface defects of asphalt pavements [25,29,63].

Haas et al. [19] were the first authors that investigated and extracted a pavement condition index (PCI) by connecting the road physical parameters (cracking, rutting and raveling) gathered from field observations with the Global Positioning System (GPS). This common technology provides detailed and geo-referenced information about road condition even though the low cost and easy managing requirements remain unsolved. Furthermore, land-based mobile mapping systems with an extensive set of sensors (including laser reflectometers, ultrasonic sensors, accelerometers, global positioning systems, gyroscopes, video and machine vision systems) and computers, such as Automated Road Analyser (developed by Roadware GRP of Paris, Ontario, Canada), have been commercially available for road mapping application [44,62]. However, the high cost of road network inspection requires the development of innovative remote sensing data analyses that are reasonably priced, easy to manage for the local authorities and valuable for the road condition mapping. For this purpose, many studies have been conducted to discriminate road surface distresses [25] and to analyze the spectral features of urban materials and their separability [4,20,22-24,51,56,58].

The characteristic absorption bands of silicates and limestone that outcrop when the asphalt pavements show surface defects, have been studied by many authors in the 8 to 12 μm thermal infrared spectral region (TIR) [32-34,53-55,65,66].

Much progress has been made in understanding the nominal range of wavelengths suitable for detecting a variety of minerals and the relationship between spectral absorption feature intensity and mineral abundance using remote sensed data [27,32,34,40,41]. Among others, the TIR spectral region is becoming increasingly more important, thus

enhancing the use of multi-channel remote sensing TIR instruments to discriminate geologic surface materials including carbonates, sulfates, clays, and felsic vs. mafic silicate minerals [3,14,49].

In this framework, the research will be focused on developing, implementing and validating the effectiveness of emission spectroscopy, in the TIR spectral range from $8.18\mu\text{m}$ to $12.70\mu\text{m}$, to provide a rapid assessment of the asphalt surface distress. Fast and non-destructive methods, such as emission spectroscopy, offer potentially useful alternatives to time-consuming chemical methods of asphalt analysis. The characteristics of asphalt pavement emissivity spectra are controlled by mineral composition, water (hydration, hygroscopic, and free pore water) and particle size distribution.

Nowadays, the most common sensors that operate in the TIR range are: the TIMS instrument ($8.2\text{--}12.6\mu\text{m}$ with 6 bands) [33], the SEBASS airborne sensor ($7.57\text{--}13.5\mu\text{m}$ with 128 bands) [36-64], the ARES instrument ($8.32\text{--}12.97\mu\text{m}$ with 32 bands) [52] and the AHI airborne sensor ($7.5\text{--}11.7\mu\text{m}$ with 256 bands) [7]. Such spectral range is covered by sensors functioning also in other spectrum regions: the DAIS-7915, the Multispectral Infrared Visible Image Spectrometer (MIVIS), the AHS-160 and the MASTER simulator ($0.46\text{--}2.39\mu\text{m}$ with 25 bands; $3.14\text{--}5.26\mu\text{m}$ with 15 bands; $7.76\text{--}12.87\mu\text{m}$ with 10 bands) [28].

In particular, the airborne MIVIS sensor, with its high spectral and/or spatial resolution [5], allows reliable quantitative measurements of specific absorption features of urban materials [1]. Moreover, a spatial resolution at least of 5m is optimum for urban applications [59,69], since "the spectral mixing space" becomes more complex with larger pixels [58,59]. Therefore, MIVIS sensor was used in order to retrieve a threshold to individuate those asphalt pavements to be checked for maintenance as it records emitted radiation in the TIR range, using a total of 10 bands with 2mrad of IFOV (Instantaneous Field Of View).

Since the asphalt pavements aging can be related to the loss of oily components [60] and to the sealing tar surface [25], and the decrease of oily components leads to an increase of several types of limestone deposits that are identifiable in the TIR range [36], a simple and fast method was developed in order to define a threshold on the basis of the band depth analysis [9] at $11.2\mu\text{m}$ (i.e., the limestone absorption peak in the TIR range).

For this purpose, an airborne MIVIS imagery covering a test area close to Venice city (Italy) was used for identifying in the TIR spectrum region the diagnostic asphalt emissivity features.

STUDY AREA

The study area (Figure 1) is characterized by a mixture of urban land cover types and surface materials, including many asphalted roads and, in particular, two main highways with asphalt pavements of different ages and conditions (i.e., more or less weathered and corroded). The study area corresponds to a MIVIS (Table 1) scene of 755 columns \times 2956 lines (Figure 1b) and is centered at latitude $45^{\circ}33'19''\text{N}$ and longitude $12^{\circ}16'49''\text{E}$. The flight strip was acquired over a rural area close to Venice city (Italy; Figure 1a) on November 23, 2006 at 11:56 (GMT), using scan rates of 25 scans/s at an altitude of 1500m, corresponding to a 3-m ground-pixel resolution at the instrument's IFOV.

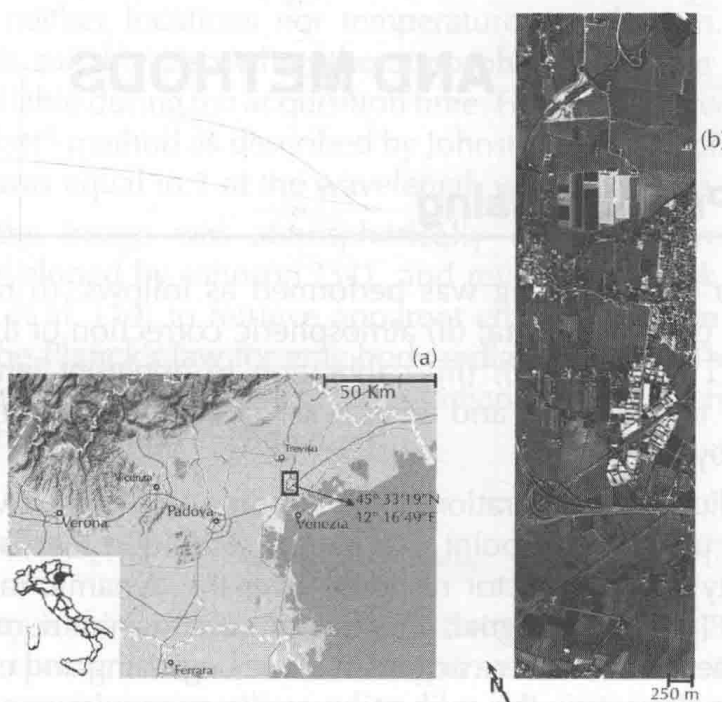


Figure 1: (a) MIVIS scene, outlined in black over a regional map; (b) MIVIS imagery acquired over Venice study area (755 columns \times 2956 lines).

Table 1: MIVIS sensor characteristics.

	VIS: 0.43-0.83 μm (channels 1-20)	Bandwidth	20 nm	SNR (min, max)	6 - 366
Spectral coverage	NIR: 1.15-1.55 μm (channels 21-28)		50 nm		80 - 1062
	SWIR: 1.98-2.47 μm (channels 29-92)		8 nm		4 - 191
	TIR: 8.18-12.70 μm (channels 93-102)		340-540 nm		150 - 1500
FOV and IFOV	71° and 2 mrad	Cross-track pixels			755
Angular	1.64	Digitalization accuracy			12 bit

DATA AND METHODS

Image Preprocessing

MIVIS data preprocessing was performed as follows: (i) radiometric calibration of the raw data; (ii) atmospheric correction of the Thermal Infra-Red (TIR) data [18]; (iii) calibration to apparent emissivity by separating temperature and emissivity according to the methods described by [16,17].

The radiometric calibration of the airborne MIVIS TIR raw data was performed using a two-point calibration technique that is based on the linearity of the detector response over the dynamic range of the instrument [47]. To this goal, the maximum and minimum reference values of the radiance were acquired at the beginning and end of each scanline to satisfy the calibration accuracy requirements.

The retrieved pixel spectral radiance ($\text{nW cm}^{-2} \text{sr}^{-1} \text{nm}^{-1}$) ($R_{\lambda}^{\text{pixel}}$), expressed by a linear equation obtained jointing the two reference points (i.e., the maximum and minimum reference values expressed by

the radiance value and the corresponding Digital Number), is shown in Equation 1.

$$R_{\lambda}^{\text{pixel}} = (B_{\lambda\text{HBB}} - B_{\lambda\text{CBB}}) \left[\frac{\text{DN}_{\lambda}^{\text{pixel}} - \text{DN}_{\lambda\text{CBB}}}{\text{DN}_{\lambda\text{HBB}} - \text{DN}_{\lambda\text{CBB}}} \right] - B_{\lambda\text{CBB}} \quad (1)$$

Where, the $\text{DN}_{\lambda}^{\text{pixel}}$ is the pixel raw data to be radiometrically calibrated; the $\text{DN}_{\lambda\text{CBB}}$ and $\text{DN}_{\lambda\text{HBB}}$ are the spectral raw data measured for the cold (minimum reference value) and hot (maximum reference value) blackbody, respectively; $B_{\lambda\text{CBB}}$ and $B_{\lambda\text{HBB}}$ are the spectral radiance values for each blackbody as predicted by Planck's law with emissivity equal to one ($\epsilon_{\lambda}=1$) and known temperature (T_i).

As regards the atmospheric attenuation of the TIR spectral radiance that includes atmospheric transmission and upwelling atmospheric radiance, the ISAC (In-Scene Atmospheric Compensation) algorithm [31,36,64,70] was employed for MIVIS TIR atmospheric correction. This algorithm assumes two pixels of the scene to be blackbodies on which neither locations nor temperatures are known. The ISAC algorithm is suitable also when the atmospheric radiative conditions are not available during the acquisition time. For this study, we followed the "most hits" method as described by Johnson [31] and pixels whose emissivity was equal to 1 at the wavelength were used as a marker.

Once the image was atmospherically corrected, we used the method developed by Johnson [31], and revised by Hook et al. [27] and Kahle et al. [34] to retrieve apparent emissivities. The method is based on the Planck's law for gray body radiator ($\epsilon_{\lambda} \neq 1$). The standard formulation of this law for the spectral radiance (L_{λ}) of each pixel (i) is described by the following equation:

$$L_{\lambda,i} = [\epsilon_{\lambda,i} B_{\lambda}(T_i) + (1 - \epsilon_{\lambda,i}) L_{\text{SKY}\lambda}] \tau_{\lambda} + L_{\text{ATM}\lambda} \quad (2)$$

where $\epsilon_{\lambda,i}$ is the surface spectral emissivity of pixel (i); $B_{\lambda}(T_i)$ is the blackbody spectral radiance at T_i temperature, located at pixel (i); $L_{\text{SKY}\lambda}$ is the spectral downwelling radiance; τ_{λ} is the spectral atmospheric transmission; $L_{\text{ATM}\lambda}$ the spectral upwelling radiance. The $L_{\text{SKY}\lambda}$ and $L_{\text{ATM}\lambda}$ are related to the emission of the atmosphere itself that

reaches directly the sensor or is reflected by the surface before being acquired by the sensor and they are also assumed to be independent from the view angle (i.e., pixel location) [36,64].

In order to extract pixel emissivity from the pixel radiance, the requirement is to discriminate from Equation (2) the emission that depends on the kinetic T and other atmospheric parameters as well as the ϵ value for each image band [16]. This multivariable problem is solved by using the assumption of ISAC algorithm about the linear relationship between the observed radiance and the Planck's function, whose slope is related to the atmospheric transmission (τ_λ), and whose offset is the upwelling atmospheric radiance ($L_{ATM\lambda}$), at that wavelength:

$$B_\lambda(T_i) = \frac{[L_{\lambda,i} - L_{ATM\lambda}]}{\tau_\lambda \epsilon_{\lambda,i}} \quad (3)$$

The emissivity can be calculated from this linear equation, in terms of the other variables:

$$\epsilon_{\lambda,i} = \frac{[L_{\lambda,i} - L_{ATM\lambda}]}{[B_\lambda(T_i) \tau_\lambda]} \quad (4)$$

Substituting in Eq. (4) the Eq. (2) and solving for T , then gives

$$T_i = \frac{C_2}{\lambda \ln[(\epsilon_{\lambda,i} C_{1\tau\lambda} / \pi \lambda^5 (L_{\lambda,i} - L_{ATM\lambda})) + 1]} \quad (5)$$

As the goal of this study is the assessment of the spectral feature shapes and the band depth analysis, we need to retrieve relative emissivities. In this context, several methods have been proposed in literature for deriving emissivities such as the reference channel method [32], the emissivity normalization method [17], the temperature-independent spectral indices [3], the thermal log residuals and alpha residuals [26], and the spectral emissivity ratios [68]. Several of these methods are compared and reviewed by Gillespie [15-17], by Hook et al. [26,27] and by Li et al. [45].

In this study we applied the emissivity normalization routine proposed by Realmuto [50], Hook et al. [26], Kealy and Hook [35] and Gu et al. [18] and implemented in the ENVI 4.4. [41] image processing software. This routine, first, derives the brightness temperature of each pixel from the pixel radiance. Afterward, the apparent emissivity image is obtained by normalizing the radiance of each pixel to the Planck's curve that is generated from the pixel with the maximum brightness temperature with an emissivity value set to 0.96 (i.e., a reasonable hypothesis for exposed mineral surfaces).

Image Classification

To develop a method for automated image analysis of road asphalt pavements on the basis of their emissivity spectral features, (a) an object-oriented approach and (b) a band-depth analysis were used (Figure 2).

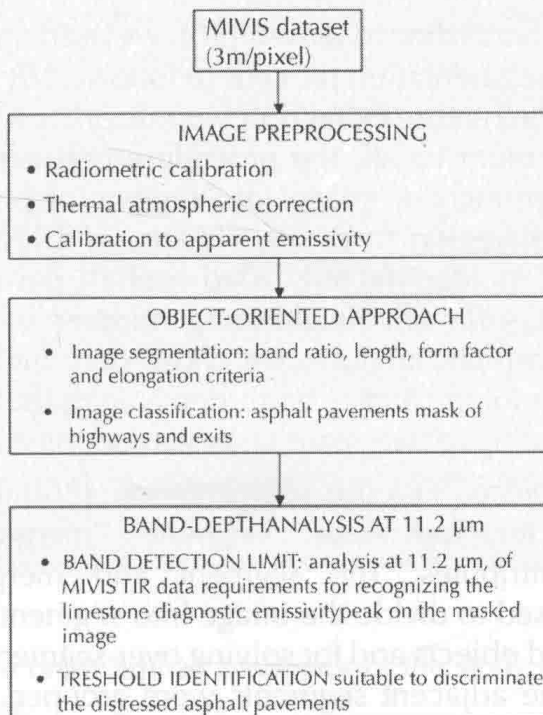


Figure 2: Flow diagram indicating the steps followed in the methods.

Object-Oriented Approach

An object-oriented approach was first adopted in order to individuate and select on MIVIS imagery the asphalt roads [6,43], which was also used as an input mask later on in the band-depth analysis.

Object-oriented approaches can represent a valuable alternative to the conventional pixel-based classification methods, as they consider the spatial context. Segmentation methods divide a study area into adjoining clusters of pixels, called segments or regions, based on similarity or dissimilarity of their single or multiple-layer pixel values [61].

The segmentation approach allows for: (a) quantifying the spatial heterogeneity within the data at various scale levels; (b) delineating homogeneous patches also involving a certain spatial generalization; (c) implementing an explicit hierarchical structure between segments at different spatial scales. As a result, spatial information is very important in classification processes to produce reliable maps [46].

For this study, according to Jensen [30], we used an object-oriented approach with a segmentation procedure followed by classification as implemented in the Feature Extraction module of the ENVI 4.4 software package [42]. In more detail, the procedure consists of a combined process of segmenting the image into regions of pixels, computing attributes for each region to create objects, and last classifying the objects. In order to identify only road asphalt pavements with the requirement of a sufficient neighboring number of pixels showing a homogeneous asphalt mixture, we chose only highways and exits asphalt pavements for the further band-depth analysis. For this purpose, a workflow consisting of two main tasks was adopted.

- (i) The *"find objects"* task (i.e. segmentation; [30]) that was divided, in its turn, into four steps: *"segment"*, *"merge"*, *"refine"*, and *"compute attributes"*. The *"segment"* and *"merge"* steps of this task were used to divide the image into segments corresponding to real-world objects and for solving over-segmentation problems and then the adjacent segments were grouped on the basis of their brightness value.
- (ii) The *"rule-based classification"* task (i.e. classification; [30]) was used to extract only the highways and exits objects and then to export them onto a raster image.

In this final step, the rules criteria with the relative appropriate scale factors (i.e., weights) were identified using both spectral and spatial attributes for classifying the highways/exits asphalt pavements objects.

Band Depth Analysis on Asphalt Roads

In Italy road paving asphalts are made of a mixture of mineral aggregate (mainly of silicates and limestone granules) and bitumen [2]. Asphalt pavements surface defects [67] are strictly related to the decrease of the oily components of the bitumen, thus increasing the surface abundance of the limestone granules (see Figure 3). Therefore, for this study we chose the outcrop of the limestone granules, which certainly highlights distressed paving asphalts, as an indicator for those asphalt pavements to be checked for maintenance.

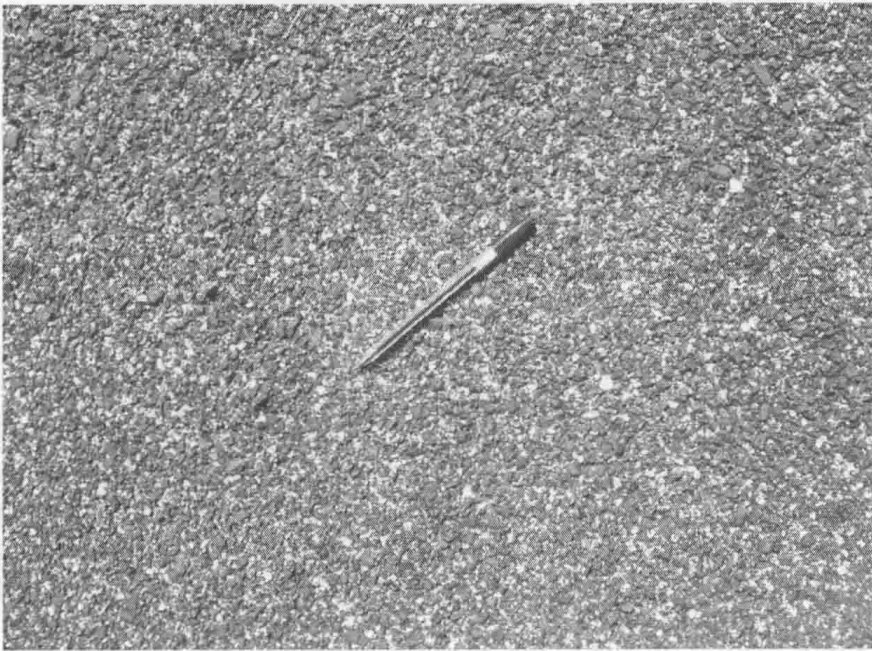


Figure 3: Example of an asphalt pavement of the study area with surfacing limestone granules.

The applied procedure consists, first, of the analysis of the available John Hopkins University (JHU) spectral library [55] information allowed for retrieving the emissivity spectral features (8-13 μ m TIR range) of